

Novel Broadband High Gain Antenna Design by Suspended Cylinder and Shorting Pin

Subash C. Yadav* and Siddhartha P. Duttagupta

Abstract—Desire for a broadband, high gain, unidirectional and low cost antenna in the field of communications is everlasting. In this paper, a novel broadband high gain antenna is presented using a suspended cylinder and a ground connected cylinder geometry. The bandwidth of the proposed antenna is enhanced by shorting these two cylinders with a pin in the direction orthogonal to the plane of coaxial probe. This low profile antenna structure is simple and easy to fabricate. The cylinders, shorting pin and ground plane are fabricated by a copper sheet of thickness 0.4 mm. Shorting pin and SMA connector provide mechanical support to the suspended cylinder. Simulations are done to analyze the radiation performance of the antenna. Prototype of the antenna is fabricated, and the measured results show good agreement with the simulated ones to confirm the enhanced bandwidth offered by the proposed antenna. We achieve impedance bandwidth of 63% (2.6–5 GHz) with the peak broadside gain of 9.87 dB. The bandwidth of the proposed antenna can be tuned by changing the radius of the shorting pin. The designed antenna possesses broadband high gain with stable broadside unidirectional radiation pattern which is suitable for Base station antenna such as WiMax (Worldwide Interoperability for Microwave Access) and LTE (Long Term Evolution). The metallic antenna has high power handling capacity as compared to microstrip and dielectric antennas. Therefore, this antenna can also be used for high power transfer application.

1. INTRODUCTION

In recent years, the design of broadband high gain, low profile antenna with unidirectional radiation pattern has been the focus of the research community because of the rapid development of modern wireless communication applications such as base station, compact handheld devices, microwave imaging, Radar, and satellite communication [1]. In all such applications, antennas with broad bandwidth, high gain and stable radiation pattern over the operating band are preferred [2]. However, for such applications, in general a microstrip antenna is used which has low bandwidth and low gain [3–5]. Recently, due to easy availability of additive manufacturing technology (AM) and three-dimensional printing technology, three-dimensional (3-D) antennas have become a popular component among research communities [6–8]. The horn antenna reported in [9] has broadband and high gain, but the design is non-planar and bulky in size, and the design requires an external feeding antenna. The Ultra Wideband Lossless Cavity-Backed Vivaldi Antenna reported in [10, 11] has broad bandwidth, and gain is higher at higher frequency, but it requires external cavity. Therefore, size is bulky, and fabrication is costly. A dual-band loop-dipole composite unidirectional antenna has been reported in [12] which has 71% and 39% impedance bandwidths at the first and second resonance frequencies, respectively. However, the gain of the antenna is low (6.5–6.7 dB), and the design is complex and costly. A differential fed wideband high gain dielectric resonator antenna reported in [13] has a peak gain of 12.2 dB and impedance bandwidth of 30%, but the fabrication cost is high because costly higher dielectric constant

Received 22 July 2018, Accepted 24 August 2018, Scheduled 6 September 2018

* Corresponding author: Subash Chandra Yadav (subashiitkgp@gmail.com).

The authors are with the Department of Electrical Engineering IIT Bombay, India.

materials have been used for fabrication. The high gain Yagi-Uda antenna with a complex reflector reported in [14] is compact, but its bandwidth is (55% 2.12–3.37 GHz), and peak gain is (5.4 dBi) low. All these reported designs require a dedicated complex fabrication procedure with high cost material. In order to solve the issue, we report a metal-only easily fabricable three-dimensional antenna. The metallic antenna has higher power handling capacity than microstrip antenna and dielectric resonator antenna [15] because of dielectric breakdown. Therefore, this antenna can be used for high power transfer applications such as base station antennas.

This paper reports a novel broadband high gain unidirectional antenna design using two cylinders and a circular reflecting ground plane. The geometry of the proposed antenna is shown in Fig. 1. The shorting pin is used to enhance the impedance bandwidth by shorting two cylinders at orthogonal point of the feed probe and is placed where the electric field is minimized at the first resonance frequency. Therefore, shorting pin does affect the first resonance, but it generates a second resonant frequency due to the enhancement of current coupling between two circumferences of the cylinders. At the second resonance, excited current flows from the suspended cylinder to the inner cylinder through the shorting pin. The shorting pin radius affects the higher resonant frequency. Therefore, by tuning the radius of the shorting pin a wide bandwidth can be achieved. High-Frequency Structure Simulator (HFSS) is used to optimize the antenna.

2. ANTENNA STRUCTURE

The structure of the proposed antenna is shown in Fig. 1, where the antenna is designed on a circular ground plane of radius ‘ R ’. A cylinder, with height ‘ H_2 ’ and radius a , is suspended at height H_3 , from the ground plane. Cylinder connected to ground has height H_1 and radius b , and a $50\ \Omega$ SMA connector is used to feed the cylinders at height h above the ground plane. Spacing between cylinders is 3.8 mm. The radius of shorting pin is r , and w is the height of coaxial probe from the bottom of the suspended cylinder.

The designed antenna, shown in Fig. 1, is excited by a coaxial probe where the first resonance frequency is generated due to circumferential current across the cylinders. The higher resonance frequency is generated due to electric field coupling between the cylinders because of shorting of the cylinders by the pin. The coupled electric field excites the current from suspended cylinder to ground connected cylinder through shorting pin. The height of the suspended cylinder is used for impedance matching at the first resonance frequency, whereas inner cylinder height and shorting pin radius change the higher resonant frequency as shown in Fig. 5 and Fig. 6. The proposed antenna is simulated by taking dimensions given in the Table 1. The simulated return loss vs. frequency graphs are shown in Fig. 2 with and without the shorting pin. The figures indicate that antenna without shorting pin has a resonance frequency of 2.6 GHz with -10 dB impedance bandwidth 23% (2.4 GHz to 3 GHz). The antenna with shorting pin does not have any impact on lower resonance frequency at 2.6 GHz, but it generates a higher resonance frequency at 4 GHz, which improves -10 dB impedance bandwidth 59% (2.4–4.6 GHz). The bandwidth of the proposed antenna with the shorting pin increases as the radius of shorted pin increases because higher resonance frequency is blue shifted. As shown in Fig. 3, there is a small improvement in broadside gain of the proposed antenna at the higher frequency due to enhancement of coupling by shorting the cylinders.

Table 1. Dimensions of antenna (All antenna dimensions are in mm).

R	H_1	H_2	h	b	a	L	w	H_3	r
70	22	14	15	17.2	21.4	24	5	10	3

Fig. 2 shows that antenna bandwidth is enhanced by shorting the cylinders (schematic shown in Fig. 1). In Fig. 3 the broadside gain of the antenna at higher frequency (4.2–5 GHz) is enhanced due to improvement of S_{11} (dB). Shorting pin enhances the coupling between the cylinders at the higher frequency band which increases the bandwidth and gain at higher frequency.

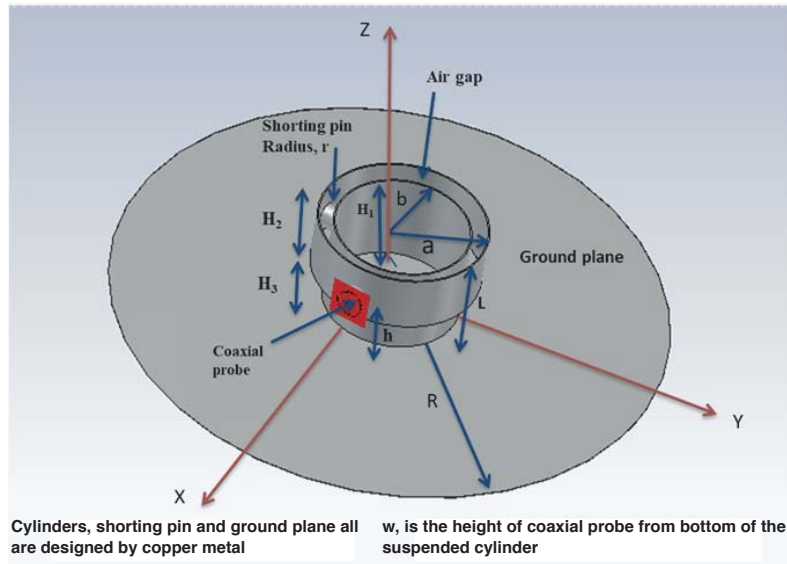


Figure 1. Schematic design of the proposed broadband high gain antenna.

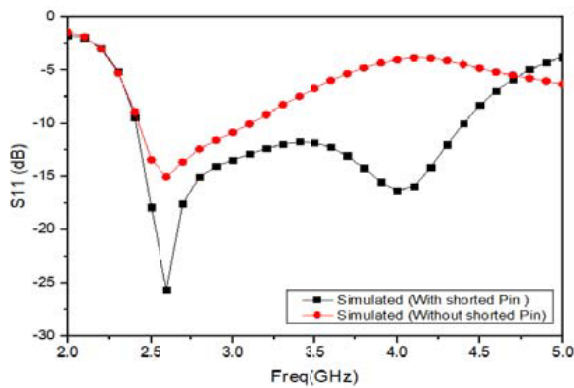


Figure 2. Simulated return loss of the proposed antenna with and without shorting pin.

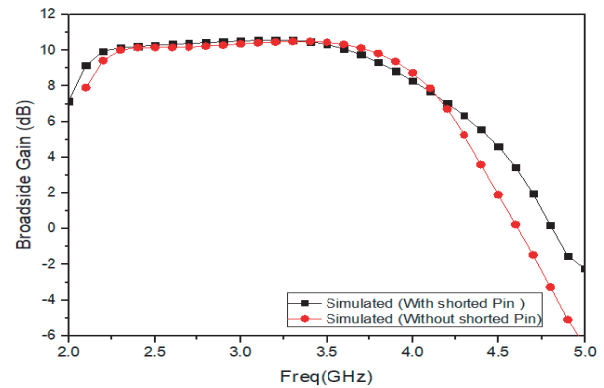


Figure 3. Simulated broadside gain of the proposed antenna with and without the shorting pin.

3. DESIGN PROCEDURE

The electric field distributions of the proposed antenna are plotted with shorting pin and without pin as shown in Fig. 4. The simulated electric field distribution of the proposed antenna without shorting pin is plotted at resonance frequency 2.6 GHz as shown in Fig. 4(a), where the electric field is maximum along the coaxial probe and minimum at orthogonal plane of the coaxial probe. If a shorting pin is placed at orthogonal plane of coaxial probe where the electric field is minimum, then it does not affect the field distribution at first resonance frequency 2.6 GHz as shown in Fig. 4(b). However, the electric field distribution is changed at higher resonance frequency 4 GHz as shown in Fig. 4(c) and Fig. 4(d). This change in field distribution creates a current through shorting pin from suspended cylinder to ground connected cylinder, and this current excites higher resonance frequency and enhances impedance bandwidth.

The electric field distribution plot in Fig. 4(a) indicates that the electric field varies across the circumference of the cylinders. Field distributions are maximum along the probe and minimum at orthogonal to the probe. There are two nodal points with a maximum and minimum across the circumference. Therefore, the first resonant frequency can be found mathematically by equating average

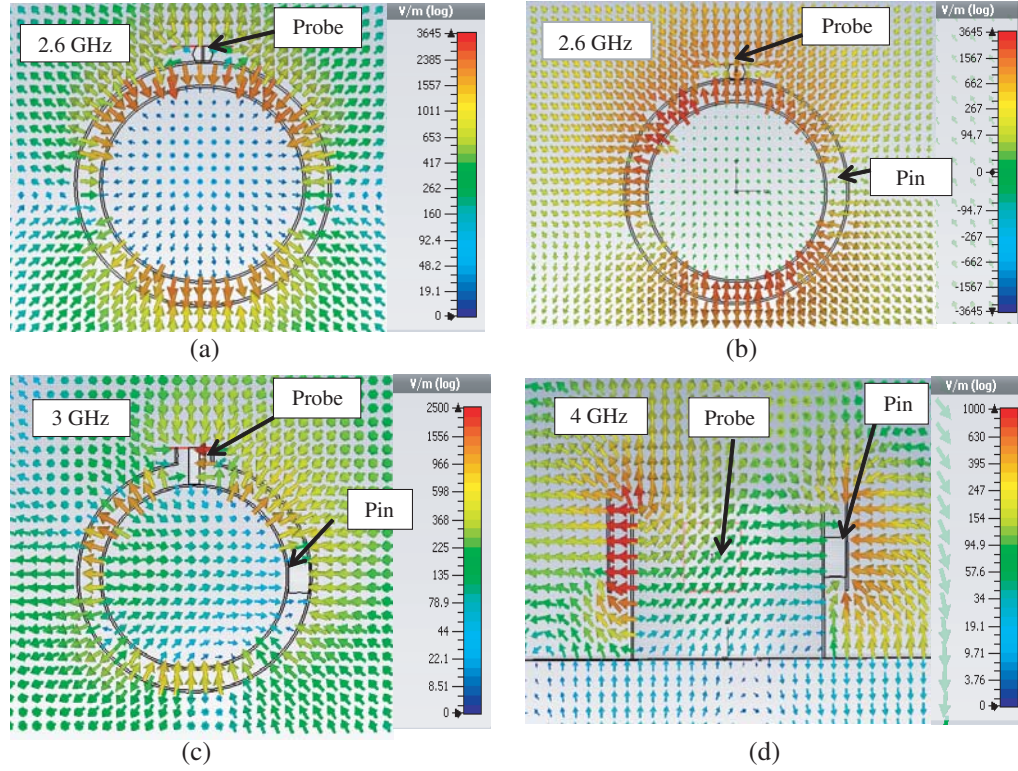


Figure 4. (a) Top view simulated electric field distribution at first resonance frequency 2.6 GHz without shorting pin. (b) Top view Simulated electric field distribution with a shorting pin at 2.6 GHz. (c) Top view of Simulated electric field distribution at second resonance frequency 4 GHz. (d) Side view of simulated electric field distribution at second resonance frequency 4 GHz.

circumference of cylinders with wavelength.

$$C_{avg} \approx \lambda \text{ or } f_{r1} \approx \frac{c}{C_{avg}} \quad (1)$$

where f_{r1} is the first resonance frequency, c the speed of light in free space and $C_{avg} \approx 2\pi\frac{(a+b)}{2}$, where a is the radius of the suspended cylinder and b the radius of the inner cylinder.

The second resonance frequency is generated due to shorting the two cylinders at orthogonal point of the coaxial probe. This shorting pin enhances electric field coupling at higher frequency as shown in Fig. 4(c) and Fig. 4(d). Thus, coupled electric field excites along the height of the inner cylinder through shorting pin. The inner cylinder has two ends. One end is connected to the ground plane, and the other end is open. Therefore, resonant height H_1 is $\lambda/4$. However, the shorting pin blocks some part of the resonant height which is equal to the diameter of the pin. Therefore, the resonant height decreases to $H_1 - 2r$, and equating this resonant height ($H_1 - 2r$) with $\lambda/4$ would give mathematical equation for the second resonance frequency.

$$f_{r2} \approx \frac{c}{4(H_1 - 2r)} \quad (2)$$

where f_{r2} is the second resonance frequency, H_1 the height of the inner cylinder, r the radius of a shorting pin, and c the speed of light in free space.

4. PARAMETRIC STUDY AND DESIGN PROCEDURE

The antenna structures are simulated by taking dimensions from Table 1, and the effects of different dimensional parameters on the resonance (at a time only one parameter is changed) of the antenna have been studied in graphs below.

The second resonance frequency of the proposed antenna is shifted by changing the radius of the shorting pin as shown in Fig. 5. As the radius of shorting pin increases, the second resonance is shifted to the higher frequency. The impedance bandwidth is increased due to coupling enhancement between the cylinders. The effect of the change in resonance frequency with respect to changes in ground connected cylinder height is studied in Fig. 6. The plots show that by reducing the height of the ground connected cylinder the second resonance is shifted to higher frequency, and thereby impedance bandwidth is increased.

The effects on broadside gain by increasing the radius of the ground plane are studied in Fig. 7. For small ground plane radius ($R = 40$ mm and 50 mm) the gain is flat over the entire impedance bandwidth. As the ground plane radius is increased, the gain at lower resonance is increased due to larger effective area. The reduction of gain in higher resonance frequency is attributed to the generation of surface wave which creates destructive interference in the broadside direction due to open ended ground plane. This antenna has capability to give a flat gain over entire impedance bandwidth or higher gain at the first resonance frequency and lower gain at the second resonance frequency. Therefore, the broadside gain of the proposed antenna is controlled by varying the size of the ground plane. The simulated antenna for $R = 80$ mm has 11 dB broadside gain at the lower frequency band, but the gain at the higher resonance frequency band is reduced.

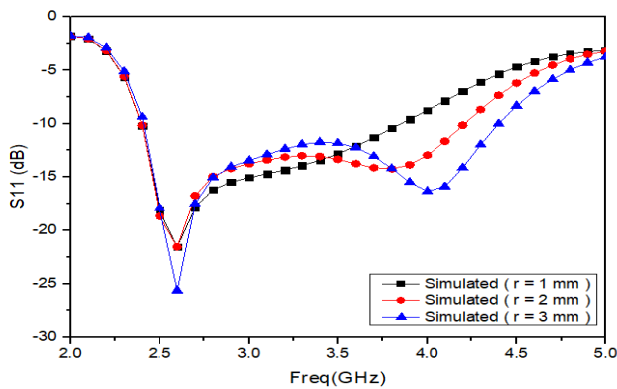


Figure 5. HFSS simulated return loss of the proposed antenna for different value of shorting pin radius.

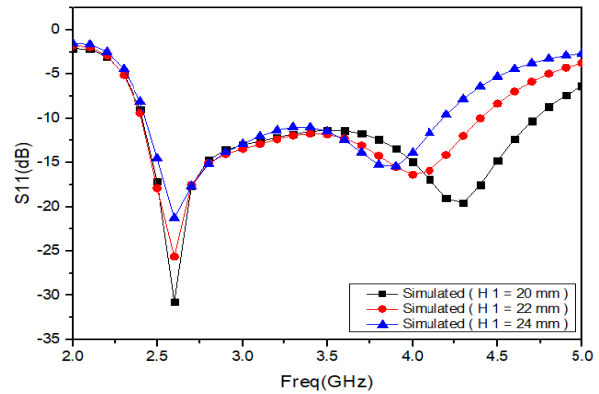


Figure 6. HFSS simulated antenna return loss for different value of inner cylinder height H_1 .

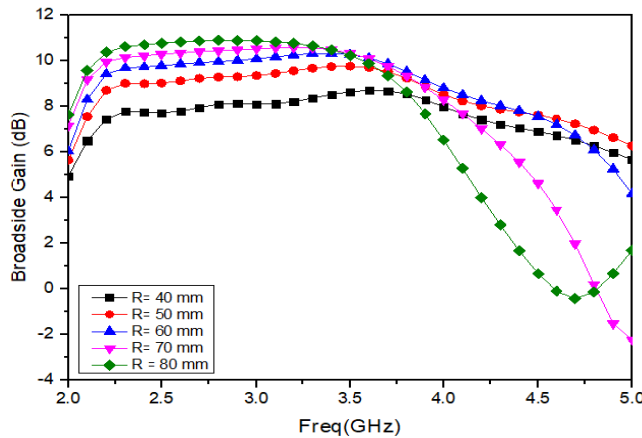


Figure 7. Simulated broadside gain of the antenna for the different ground plane radius.

5. FABRICATION, RESULTS, AND DISCUSSIONS

The prototype of the proposed antenna is shown in Fig. 8 where a copper sheet of thickness 0.4 mm is used to make cylinders, shorting pin and ground plane. The spacing between the cylinders is 3.8 mm. In this fabrication process copper sheet is folded in cylindrical shape, and then soldering is done to join different parts. The ground plane is simply created by the cutting the copper sheet, and it is stuck on hard paper for providing support as shown in Fig. 8(b). The shorting pin is also designed with a folding copper foil in cylindrical form. The SMA connector and shorting pin provide mechanical support to the suspended cylinder. Therefore, no external component is required to suspend the outer cylinder. The antenna is designed by taking dimensions from Table 1.

The comparison between measured and simulated return losses and broadside gains of the fabricated antenna are shown in Fig. 9 & Fig. 10, respectively. The HFSS simulated antenna has impedance bandwidth 59% (2.4–4.6 GHz) with peak gain 10.5 dB whereas fabricated antenna has impedance bandwidth of 63% (2.6–5 GHz) and peak gain 9.87 dB. The small differences between simulated and measured results are attributed to the mismatch between simulated dimensions and actual fabricated dimensions which arises from fabrication error. The peak gain of the proposed antenna is smaller than simulated antenna due to losses in copper and manufacturing errors. The comparisons of simulation and

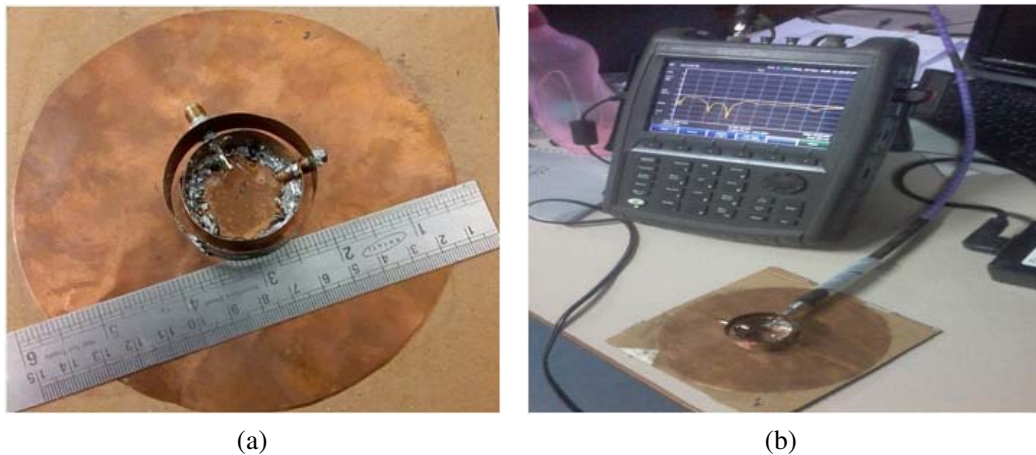


Figure 8. Fabricated antenna by taking dimensions from Table 1. (a) Top view of the fabricated antenna. (b) Measurement setup of the proposed antenna with a frequency sweep from (1–10 GHz).

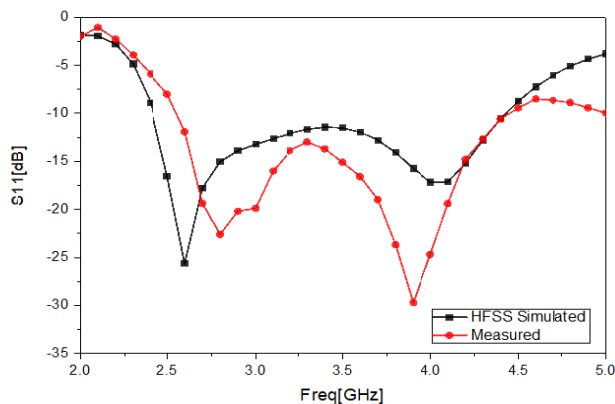


Figure 9. Simulated and measured return loss of the proposed antenna.

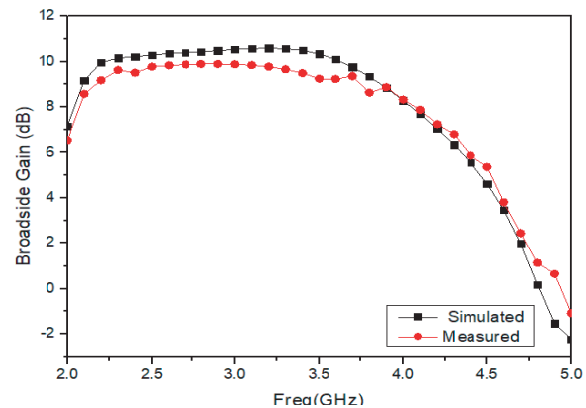


Figure 10. Simulated Gain vs. frequencies in broadside-maximum Gain is 10 dB.

Table 2. Comparisons of simulated and measured results.

Parameters	HFSS (Simulated)	Measured
Resonant Frequency	$f_{r1} = 2.6 \text{ GHz}$ $f_{r2} = 4 \text{ GHz}$	$f_{r1} = 2.75 \text{ GHz}$ & $f_{r2} = 3.9 \text{ GHz}$
Impedance Bandwidth	59% at 3.5 GHz (2.4–4.6 GHz)	63% at 3.8 GHz (2.6–5 GHz)
Peak Gain (Broadside)	10.5 dBi	9.87 dBi

measured results are shown in Table 2. The 3-D radiation pattern of the proposed antenna is plotted using CST, shown in Fig. 11 for different frequencies over the impedance bandwidth. The plotted radiation pattern shows a stable unidirectional radiation pattern.

Table 3 shows the comparison between proposed antennas and previously reported broadband high-gain antennas where the dimensions of the antenna are measured in terms of their wavelength (λ) corresponding to the center frequency. The proposed antenna has higher gain than that of the antennas reported in [13, 16, 18, 20]. Moreover, fabrication method of the proposed antenna is simple and less costly. The proposed antenna is compact in size as compared to [16, 17, 19, 20]. The bandwidth of the proposed antenna is better than the antenna reported in [17–20]. The shorting pin used in this antenna makes the antenna tunable at a higher resonance frequency as shown in Fig. 5. The radius of shorting

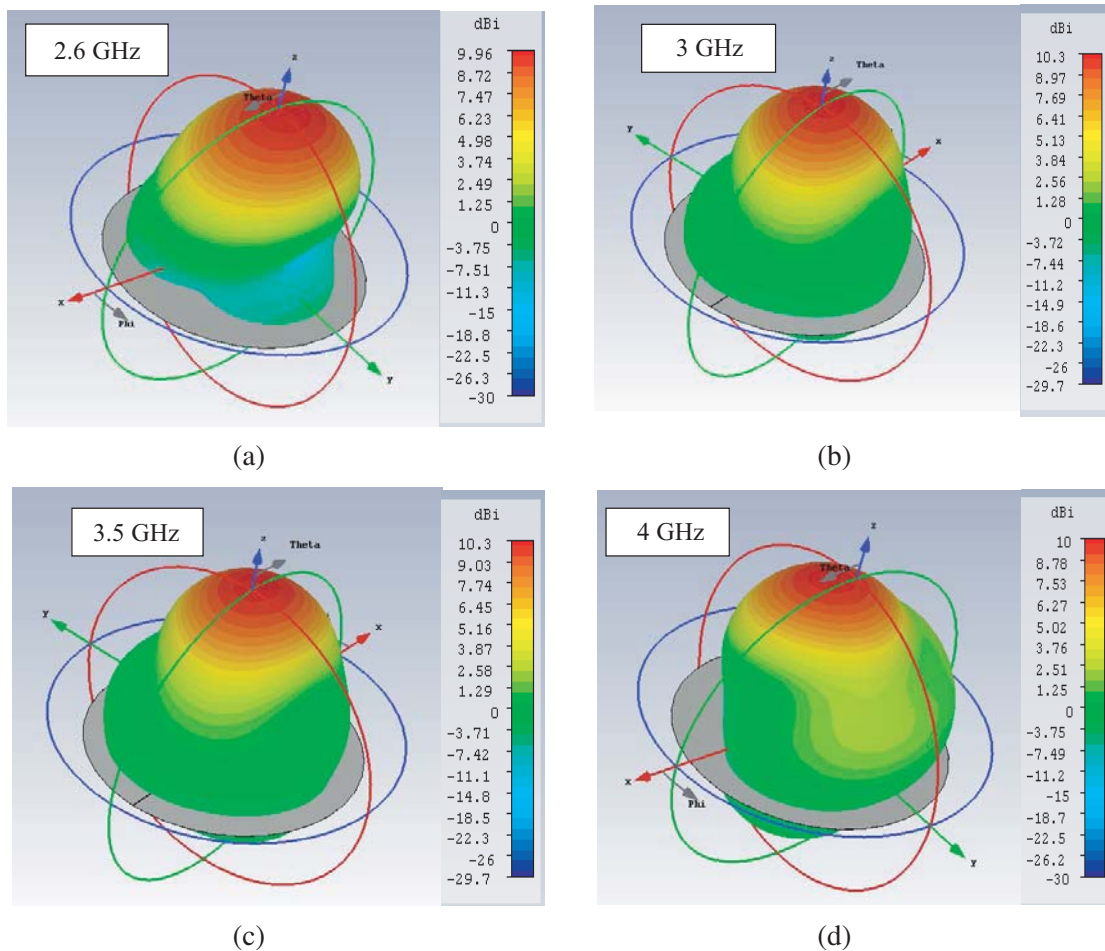


Figure 11. Simulated antenna, 3D Radiation pattern at (a) 2.6 GHz, (b) 3 GHz, (c) 3.5 GHz and (d) 4 GHz.

pin can be used to tune the higher resonance frequency. In Fig. 7 it is clearly shown that the gain of the antenna at the first resonance frequency can be improved by increasing the ground plane radius. For $R = 80$ mm, the broadside peak gain is 11 dB, but we need a compromise with the gain at the second resonance frequency. The flat gain response more than 7.5 dB is achieved for $R = 40$ mm for $R = 50$ mm, over the entire bandwidth. The designed antenna has better 1 dB gain bandwidth than the reported antennas except the antenna reported in [18]. However, the gain of the proposed antenna is better than the antenna reported in [18].

Table 3. Comparisons of proposed broadband high gain antenna from previously reported antenna in references.

	Total planner area	Total Height	-10 dB Impedance Bandwidth	Peak Gain	1 dB Gain Bandwidth	Technology
REF [12]	$1.121\lambda^2$ & $6.69\lambda^2$	0.557λ & 1.36λ	70% (1.54–3.24) GHz & 34% (4.88–6.80) GHz	(6.5–6.7) dBi	21% (1.7–2.1) GHz & 22% (2.4–3) GHz & 10.5% (5.6–6) GHz	Loop dipole composite
REF [16]	$3.725\lambda^2$	0.34λ	66.6% (2–4) GHz	9.5 dBi	11.3% (2.5–2.8) GHz	Origami
REF [17]	$3.85\lambda^2$	0.39λ	41% (1.71–2.59) GHz	11.8 dBi	16.5% (1.7–2) GHz	Frequency selective Reflector
REF [18]	$1.18\lambda^2$	0.235λ	46% (1.68–2.68) GHz	7.57 dB	74% (1.6–3) GHz	Dipole Quasi Yagi
REF [19]	$4.92\lambda^2$	0.13λ	9% (5.58–6.03) GHz	10 dB	6.8% (5.6–6) GHz	Substrate integrated waveguide & Metamaterial
REF [20]	Infinite ground plane	1.666λ	1.2% (4.95–5) GHz	8 dB	1.2% (4.95–5) GHz	Stub Loaded Monopole
This work	$2.47\lambda^2$	0.304λ	63% (2.6–5) GHz	9.87 dB	48.7% (2.3–3.8)	Suspended cylinder and shorting pin

6. CONCLUSION

In this paper, a novel broadband high gain antenna with a stable broadside radiation pattern is designed using suspended cylinder and shorting pin geometry. The proposed simulated antenna obtains a broad bandwidth of 59% (2.4–4.6 GHz) with peak broadside gain of 10.5 dB. The fabricated antenna obtains a broad bandwidth of 63% (2.6–5 GHz) with the peak broadside gain 9.87 dB. Thus the simulated and measured results are in good agreement. The impedance bandwidth of the proposed antenna is enhanced using a shorting pin. The structure of the proposed antenna is simple and fabricated with low cost as it requires only copper sheet of thickness 0.4 mm as a metal and a 50 Ω SMA connector. The effect of antenna dimensions on resonance frequency has been studied using simulation. The change in bandwidth and shift of the resonance frequency of the designed antenna is shown in details. The bandwidth and higher resonance frequency of the proposed antenna are mechanically tunable by changing the radius of the shorting pin. The gain of the proposed antenna can be adjusted as per requirements. We can design flat gain over the entire bandwidth by reducing the ground plane size as shown in Fig. 7, or we can make high gain at the first resonance frequency by compromising the gain at the higher resonance frequency. In the future work we can improve broadside gain at higher resonance frequency by reducing surface wave by electromagnetic band-gap structures reported in [21, 22] or using metamaterials trephines reported in [23, 24]. The gain at higher resonance frequency can be improved by flaring the ground plane in conical shape, but it increases antenna size.

REFERENCES

1. Chen, Z. N., W. Liu, and X. Qing, "Low-profile broadband mushroom and metasurface antennas," *International Workshop on Antenna Technology: Small Antennas, Innovative Structures, and Applications (iWAT)*, 1–4, Athens, Greece, March 2017.
2. Prasad, C. S. and A. Biswas, "Planar excitation of dielectric waveguide antenna for broadband and high-gain application," *IEEE Antenna and Wireless Propagation Letters*, Vol. 16, 1209–1212, 2017.
3. Balanis, C. A., *Antenna Theory: Analysis and Design*, 3rd Edition, 811, John Wiley & Sons, New York, 2011.
4. Baheti, H., D. Kumar Pathak, and U. K. Kommuri, "Broadband and high gain low profile(thin) capacitive-coupled microstrip antennas for wireless applications," *Annual IEEE India Conference (INDICON)*, 1–4, December 2015.
5. Özden, O., M. Karaaslan, E. Ünal, and D. Kapusuz, "Multistrip monopole antenna for UWB applications," *IEEE Signal Processing and Communications Applications Conference (SIU)*, 1–4, 2012.
6. Liang, M., J. Wu, X. Yu, and H. Xin, "3D printing technology for RF and THz antennas," *IEEE International Symposium on Antennas and Propagation (ISAP)*, 536–537, Japan, October 2016.
7. Garcia, C. R., R. C. Rumpf, H. H. Tsang, and J. H. Barton, "Effects of extreme surface roughness on 3D printed horn antenna," *Electronics Letters*, Vol. 49, No. 12, 734–736, June 2013.
8. Pattanayak, A., S. Roy, G. Rana, S. P. Duttgupta, V. G. Achanta, and S. S. Prabhu, "Study of plasmon hybridization of a loop Yagi-Uda absorber," *Scientific Reports*, Vol. 7, 16961, 2017.
9. Criollo, E. H. and C. I. Páez, "Improved broadband double ridged horn antenna without split radiation pattern," *IEEE Latin America Transactions*, Vol. 14, No. 3, 1156–1161, March 2016.
10. Lim, T. H., J.-E. Park, and H. Choo, "Design of the Vivaldi-fed hybrid horn antenna for low frequency gain enhancement," *IEEE Transactions on Antennas and Propagation*, Vol. 66, No. 1, 438–443, January 2018.
11. Tianang, E. G., M. A. Elmansouri, and D. S. Filipovic, "Ultra-wideband lossless cavity-backed Vivaldi antenna," *IEEE Transactions on Antennas and Propagation*, Vol. 66, No. 1, 115–124, January 2018.
12. Lu, W.-J., G.-M. Liu, K. F. Tong, and H.-B. Zhu, "Dual-band loop-dipole composite unidirectional antenna for broadband wireless communication system," *IEEE Transactions on Antennas and Propagation*, Vol. 62, No. 5, 2860–2866, May 2014.
13. Gupta, R. D. and M. S. Parihar, "Differentially fed wideband rectangular DRA with high gain using short horn," *IEEE Antenna and Wireless Propagation Letter*, Vol. 16, 1804–1807, 2017.
14. Liu, L., S. Lin, A. Denisov, D. Liang, Y. Cao, and S. Tian, "A broadband and high gain yagi antenna with complex parabolic boundary reflector," *2017 IEEE International Symposium on Antennas and Propagation & USNC/URSI National Radio Science Meeting*, 1785–1786, 2017.
15. Zhang, H.-Y., F.-S. Zhang, and F. Zhang, "A novel high-gain cavity slot antenna based on polarization twist reflector for high power microwave application," *Progress In Electromagnetics Research C*, Vol. 76, 23–31, 2017.
16. Shah, S. I. H., D. Lee, M. M. Tentzeris, and S. Lim, "A novel high-gain tetrahedron origami," *IEEE Antennas and Wireless Propagation Letters*, Vol. 16, 848–851, 2017.
17. Kim, D. and E. Kim, "A high-gain wideband antenna with frequency selective side reflectors operating in an anti-resonant mode," *IEEE Antennas Wireless Propagation Letter*, Vol. 14, 442–445, 2015.
18. Yeo, J. and J.-I. Lee, "Bandwidth enhancement of double-dipole Quasi-Yagi antenna using stepped slot line structure," *IEEE Antennas and Wireless Propagation Letters*, Vol. 15, 694–697, 2016.
19. Jiang, Z. H., Q. Wu, D. E. Brocker, P. E. Sieber, and D. H. Werner, "A low-profile high-gain substrate-integrated waveguide slot antenna enabled by an ultrathin anisotropic zero-index metamaterial coating," *IEEE Transactions on Antennas and Propagation*, Vol. 62, No. 3, 1173–1184, March 2014.

20. Werner, P. L., Z. Bayraktar, B. Rybicki, D. H. Werner, K. J. Schlager, and D. Linden, "Stub-loaded long-wire monopoles optimized for high gain performance," *IEEE Transactions on Antennas and Propagation*, Vol. 56, No. 3, 639–644, March 2008.
21. Karaaslan, M., E. Ünal, E. Tetik, K. Delihacioglu, F. karadag, and F. Dincer, "Low profile radiation enhancement with novel electromagnetic band gap structure," *IET Microwave, Antennas & Propagation*, Vol. 7, 215–221, January 2013.
22. Oh, K.-H. and J.-I. Song, "Investigation of surface-wave reduction in UC-PBG patch antenna by using a transient electrooptic near-field mapping technique," *IEEE Transactions on Antennas and Propagation*, Vol. 54, No. 12, 3602–3607, December 2006.
23. Dincer, F., M. Karaaslan, M. Bakır, O. Akgol, E. Unal, K. Delihacioglu, and C. Sabah, "Increasing bandwidth in antenna applications By using chiral metamaterials," *IEEE Signal Processing and Communications Applications Conference (SIU)*, 316–318, 2015.
24. Ozturk, M., U. K. Sevim, O. Akgol, E. Unal, and M. Karaaslan, "Determination of physical properties of concrete by using microwave nondistructive technique," *ACES Journal*, Vol. 33, No. 3, March 2018.